

# Kelvin-Helmholtz instability simulation in the context of adaptive multiresolution analysis

Anna Karina Fontes Gomes<sup>1</sup>

Pós-graduação em Computação Aplicada, INPE, São José dos Campos, SP

Margarete Oliveira Domingues<sup>2</sup>

Laboratório Associado de Computação e Matemática Aplicada, INPE, São José dos Campos, SP

Odim Mendes<sup>3</sup>

Divisão de Geofísica Espacial, INPE, São José dos Campos, SP

**Abstract** This work is concerned with the numerical simulation of the Kelvin-Helmholtz instability using a two-dimensional ideal magnetohydrodynamics model in the context of adaptive multiresolution approach. The Kelvin-Helmholtz instabilities are caused by a velocity shear and normally expected in a layer between two fluids with different velocities. Due to its complexity, this kind of problem is a well-known test for numerical schemes and it is important for the verification of the developed code. The aim of this paper is to compare our solution with the solution of the well known astrophysics FLASH code to verify our code in respect to this reference.

**Keywords.** Magnetohydrodynamics, Kelvin-Helmholtz instability, Adaptive multiresolution analysis, Numerical simulation

## 1 Introduction

The magnetohydrodynamics (MHD) theory describes the dynamics of a conducting fluid in presence of magnetic fields and constitutes an important tool to study the macroscopic behavior of plasmas. In this context, the Kelvin-Helmholtz instability, which is commonly expected in boundary layers separating two fluids, is an important and a complex physical problem that can be studied with the MHD models, and should often occur in both astrophysical and space geophysical environments [4]. On the discretization of the MHD system, we use a finite volume method combined with an adaptive multiresolution (MR) approach to create a computational mesh refined where local structures are presented. The MR for cell-averages was firstly introduced by Ami Harten [8] and its idea is to represent a set of data in different levels of resolution by using a wavelet transform. The MR algorithm is implemented for compressible Navier-Stokes and 5 more system of equations in the  $C^{++}$  code named CARMEN [12]. The ideal MHD equations were added later to the CARMEN code [2, 6, 7], and it is employed herein.

---

<sup>1</sup>anna.gomes@inpe.br

<sup>2</sup>margarete.domingues@inpe.br

<sup>3</sup>odim.mendes@inpe.br

We use the well-known in astrophysics and space geophysics FLASH code [5], developed by the Flash Center in University of Chicago, to create a reference MHD solution to our results. The goal of this work is to verify the numerical results of CARMEN code for the Kelvin-Helmholtz instability problem by comparing them with the reference solution, which is obtained in a regular cartesian mesh.

The content is organized as follows. In Section 2, we briefly present the MHD model and the MR approach we use to simulate the Kelvin-Helmholtz instabilities. In Section 3, the numerical results and discussion are shown. The final remarks are presented in Section 4.

## 2 Methodology

In this section, we introduce the MHD equations and the multiresolution approach used in the numerical experiments. The ideal MHD model is given by

$$\frac{\partial \rho}{\partial t} + \nabla \cdot (\rho \mathbf{u}) = 0, \tag{1a}$$

$$\frac{\partial e}{\partial t} + \nabla \cdot \left[ \left( e + p + \frac{\mathbf{B} \cdot \mathbf{B}}{2} \right) \mathbf{u} - \mathbf{B} (\mathbf{u} \cdot \mathbf{B}) \right] = 0, \tag{1b}$$

$$\frac{\partial (\rho \mathbf{u})}{\partial t} + \nabla \cdot \left[ \rho \mathbf{u}^t \mathbf{u} + \mathbf{I} \left( p + \frac{\mathbf{B} \cdot \mathbf{B}}{2} \right) - \mathbf{B}^t \mathbf{B} \right] = \mathbf{0}, \tag{1c}$$

$$\frac{\partial \mathbf{B}}{\partial t} + \nabla \cdot [\mathbf{u}^t \mathbf{B} - \mathbf{B}^t \mathbf{u}] = \mathbf{0}, \tag{1d}$$

where  $\rho$  represents density,  $p$  the pressure,  $\mathbf{u} = (u_x, u_y, u_z)$  the velocity vector,  $\mathbf{B} = (B_x, B_y, B_z)$  the magnetic field vector,  $\mathbf{I}$  the identity tensor of order 2, and  $\gamma$  the ratio of specific heats ( $\gamma > 1$ ). The pressure is given by the constitutive law  $p = (\gamma - 1) \left( e - \rho \frac{\mathbf{u} \cdot \mathbf{u}}{2} - \frac{\mathbf{B} \cdot \mathbf{B}}{2} \right)$ , where  $e$  is the energy density. The ideal MHD equations describe the conservation of mass, energy, momentum and magnetic flux, respectively.

### 2.1 Numerical aspects

This MHD system can be written as a conservation law in the form

$$\frac{\partial \mathbf{U}}{\partial t} + \nabla \cdot \mathcal{F}(\mathbf{U}) = \mathcal{S}(\mathbf{U}), \tag{2}$$

where  $\mathbf{U} = (\rho, e, \mathbf{u}, \mathbf{B})$  is the vector of conservative variables,  $\mathcal{F} = \mathcal{F}(\mathbf{U})$  and  $\mathcal{S} = \mathcal{S}(\mathbf{U})$  are the flux and source term vectors.

The magnetic field divergence constraint  $\nabla \cdot \mathbf{B} = 0$  is not satisfied numerically, and it can lead to unphysical behavior in the numerical solution of the MHD model. Thus it is necessary to avoid the generation of numerical errors by adding a correction to the system, which prevent magnetic monopoles in the solution of the model. Two-techniques are proposed to reduce that effect:

1. **Eight-wave MHD model (FLASH code)** It uses the 8-wave source-term approach proposed by [11], which stabilizes the numerical method by adding source

terms proportional to  $\nabla \cdot \mathbf{B}$  on the right-hand side of the system, *i.e.* the source term vector  $\mathcal{S} = (0, -\mathbf{B}\nabla \cdot \mathbf{B}, -\mathbf{u}\nabla \cdot \mathbf{B}, -(\mathbf{u} \cdot \mathbf{B})\nabla \cdot \mathbf{B})$  is added to the MHD equations.

2. **Generalized Lagrange Multiplier MHD model (CARMEN code)** It uses the ideal MHD model with Generalized Lagrange Multiplier (GLM-MHD) with a parabolic-hyperbolic correction [1]. This divergence cleaning approach does not guarantee null divergence, but it prevents magnetic monopoles to occur by propagating and dissipating the divergence errors. In this case we introduce a new scalar variable  $\psi$ , by adding the term  $\nabla\psi$  to the left-hand side of the Equation 1d and defining a new equation to the ideal MHD system

$$\frac{\partial\psi}{\partial t} + c_h^2 \nabla \cdot \mathbf{B} = -\frac{c_h^2}{c_p^2} \psi, \quad (3)$$

where  $c_p$  and  $c_h$  are the parabolic-hyperbolic parameters, with  $c_h > 0$ , defined as  $c_h = c_h(t) := \nu_{CFL} \frac{\min\{\Delta x, \Delta y\}}{\Delta t}$ , where the Courant number  $\nu_{CFL} \in (0, 1)$ ,  $\Delta x$  and  $\Delta y$  are the space steps and  $\Delta t$  is the time step. We also consider the parameter  $\alpha = \Delta h c_h / c_p^2$ , where  $\Delta h = \min(\Delta x, \Delta y)$  [9].

**Finite volume context.** The two numerical models use the finite volume method to discretize the MHD equations, in which the domain is partitioned into cells (or volumes). This method is based on the integral form of the conservation laws and ensures the conservation of the system. To compute the flux  $\mathcal{F}$  through the cell interfaces, we use the Harten-Lax-van Leer Discontinuities (HLLD) Riemann solver [10] due its efficiency to resolve isolated discontinuities, and assure the  $2^{nd}$ -order in space with the monotonized central (MC) reconstruction [13], in both codes.

**MR method based in an adaptive cell average approach as discussed in [7, 8]** . Applying the multiresolution transform in the cell averages, we decompose them into different refinement levels and, from that, we obtain the local approximation error between the levels. These errors are called details or wavelet coefficients. The idea of adaptivity starts from the wavelet coefficients, which can measure the local regularity of the data according to a given threshold parameter  $\epsilon^\ell = \epsilon(\epsilon^0, \ell)$ , where  $\ell$  denotes the cell scale level and  $\epsilon^0$  is the initial threshold parameter. When the details are larger than  $\epsilon^\ell$  the computational mesh needs to be more refined locally; otherwise the mesh can remain coarser. This methodology allows the computational mesh to be more refined merely where it is required. In this work, we take into account the level-dependent and constant threshold parameters, in which the first varies with the level  $\ell$  and the other one remains unchanged for every  $\ell$ , with  $0 \leq \ell \leq L - 1$ . The number of cells on the finest grid is defined as  $2^{2L}$ , where  $L$  the finest scale level.

**Time evolution.** In both models the simulation is evaluated with a  $2^{nd}$ -order method. In CARMEN code, we have a compact Runge-Kutta, while in FLASH code a one-step Hancock is used. The system is completed by suitable initial and boundary conditions and the two-dimensional form of this system is considered.

### 3 Numerical Experiment

In fluids or plasmas, Kelvin-Helmholtz instability is triggered by a velocity shear as discussed, for instance, in [4]. In our simulations, we consider the initial conditions presented in Table 3, with

$$u_x^0 = 5(\tanh(20(y + 0.5)) - (\tanh(20(y - 0.5)) + 1)),$$

$$u_y^0 = 0.25 \sin(2\pi x)(\exp[-100(y + 0.5)^2] - \exp[-100(y - 0.5)^2]),$$

and the boundary condition periodic everywhere. The computational domain is  $\Omega = [0, 1.0] \times [-1.0, 1.0]$  and the finest scale is  $L = 9$ , *i.e.* a  $512 \times 512$  mesh. We also define as parameters the Courant number  $\nu_{CFL} = 0.4$ ,  $\gamma = 1.4$  and the physical time  $t = 0.5$ . For the divergence-cleaning we have  $\alpha = 0.4$ .

Table 1: Kelvin-Helmholtz instability initial condition.

$\rho$	$p$	$u_x$	$u_y$	$u_z$	$B_x$	$B_y$	$B_z$
1.0	50.0	$u_x^0$	$u_y^0$	0.0	1.0	0.0	0.0

For the MR approach, we have the threshold parameters  $\epsilon^0 = 0.1$ ,  $\epsilon^0 = 0.5$ ,  $\epsilon = 0.25$  and  $\epsilon = 0.5$ .

In the following, we present the results obtained with FLASH and CARMEN codes for this Kelvin-Helmholtz instability problem. The graphical representation of the solution obtained with both FLASH (left) and CARMEN (right) codes are presented for the variable  $\rho$  in Figure 1. Figure 2 presents the cuts for the variable  $\rho$  in  $x = 0.5$  and  $y = 0.5$ , for  $\epsilon = 0.25$  at  $t = 0.5$ . The results are very similar and they are limited by the same maximum and minimum values.

The cuts at  $x = 0.5$  and  $y = 0.5$  are the most critical in the simulation domain, due to many discontinuities located. According to Figure 2, the solution obtained with the GLM-MHD model approaches to the FLASH code solution. It also happens to the other MHD variables for every choice of  $\epsilon^0$  and  $\epsilon$  we use here. The adaptive meshes at times  $t = 0.0$ ,  $t = 0.25$  and  $t = 0.5$  are presented for  $\epsilon = 0.25$  in Figure 3. In this simulation the use of memory (percentage of cells) over time is 26% when compared to a uniform grid. This percentage increases when the level-dependent threshold is used, because of its adaptivity at each level of refinement that demands more cells to evaluate the solution, *e.g.* the percentage of memory for  $\epsilon^0 = 0.5$  is 52%. Table 2 shows the norm  $L_1$ ,  $L_\infty$  and  $L_2$  values for the variable  $\rho$  when the solution is compared with the reference. For the level-dependent threshold parameter the norms are slightly smaller than the constant parameter approach. The values for  $\epsilon = 0.25$  and  $\epsilon^0 = 0.5$  remains very close, indicating similar accuracy even for different memory use.

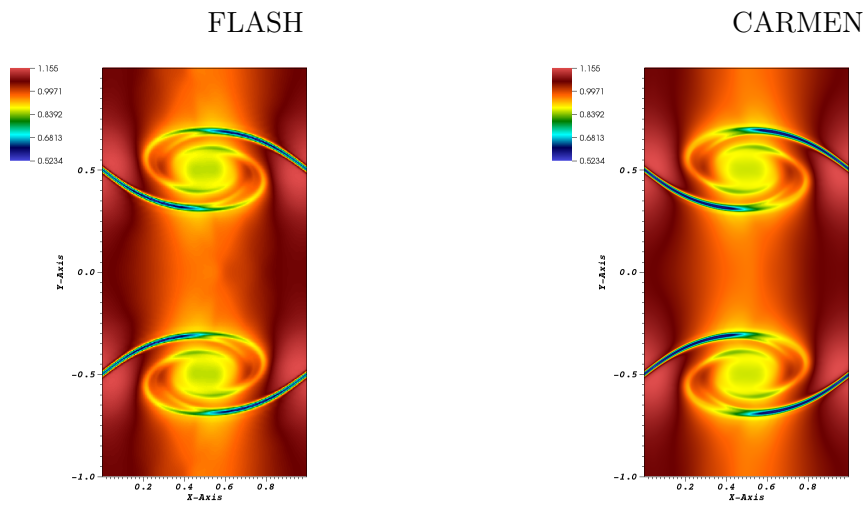


Figure 1: Variable  $\rho$  obtained at  $t = 0.5$  and  $L = 9$ , with FLASH and CARMEN codes for  $\epsilon = 0.25$ .

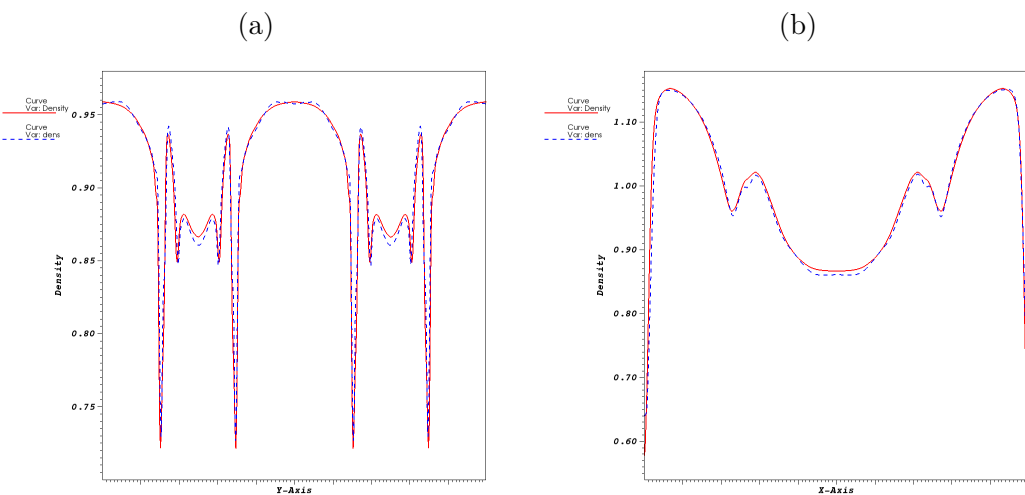


Figure 2: Cuts of variable  $\rho$  obtained at  $t = 0.5$  and  $L = 9$ , with FLASH code (blue) and CARMEN code (red) for  $\epsilon = 0.25$ , on (a)  $x = 0.5$  and (b)  $y = 0.5$ .

Table 2: Norms  $L_1$ ,  $L_\infty$  and  $L_2$  of the variable  $\rho$  for  $\epsilon^0$  and  $\epsilon$ .

	$\epsilon^0$		$\epsilon$	
	0.1	0.5	0.25	0.5
$L_1 (10^{-3})$	2.831	3.033	4.113	5.651
$L_\infty (10^{-1})$	0.878	1.365	1.438	1.318
$L_2 (10^{-5})$	1.492	1.631	1.930	2.800

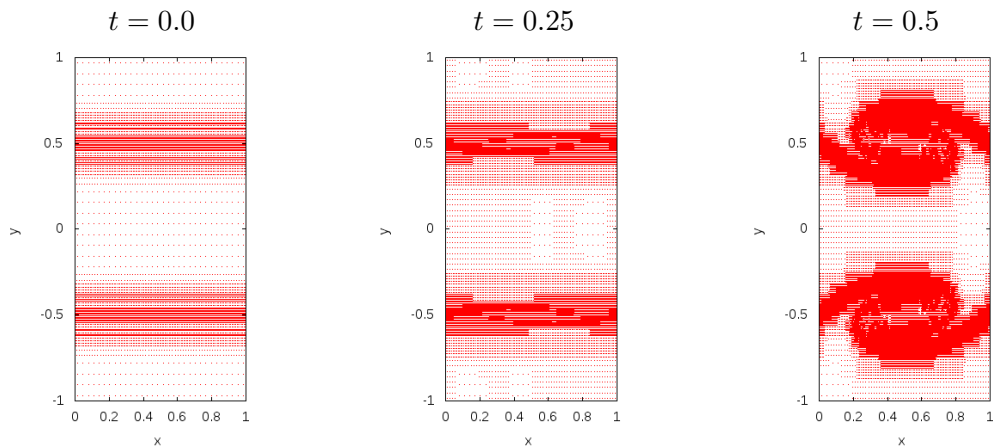


Figure 3: Adaptive MR mesh at  $t = 0.0$ ,  $t = 0.25$  and  $t = 0.5$  obtained with CARMEN code with  $\epsilon = 0.25$ .

## 4 Final Remarks

We presented a wavelet based MR approach to compute the Kelvin-Helmholtz instabilities with the GLM-MHD system and compared its results to those obtained with FLASH code. It was shown that the solution of the problem achieved with the adaptive MR is very close to the reference solution, and by taking cuts in the domain and the norm values we ensure that it leads to the expected solution. The adaptive method proved to be efficient to keep the accuracy of the solution even decreasing the number of cells in the simulation. We conclude that the presented methodology is relevant in this instability context and interesting to be extended to more complex space physics problems in future works.

## Acknowledgements

M. O. D. and O. M. thankfully acknowledge financial support from MCTI/ FINEP /INFRINPE-1 (grant 01.12.0527.00), CNPq (grants 30603-8/2015-3, 31224-6/2013-7) and FAPESP (grants 2015/25624-2). A. G. thankfully acknowledges financial support for her Master, MCTI/INPE-PCI and PhD scholarships from CNPq (grants 132045/2010-9, 312479/2012-3, 141741/2013-9). The software used in this work was in part developed by the DOE NNSA-ASC OASCR Flash Center at the University of Chicago. We also want to thank to Dr. Edgard Evangelista (CNPq-PDJ 158967/2014-3) for his help with FLASH code and Eng. Varlei Menconi (MCTI/INPE-PCI 455097/2013-5) for the computational assistance.

## References

- [1] A. Dedner, F. Kemm, D. Kröner, C.-D. Munz, T. Schnitzer, and M. Wesenberg. Hyperbolic divergence cleaning for the MHD equations. *Journal of Computational Physics*, vol. 175, 645–673, (2002).

- [2] M. O. Domingues, A. K. F. Gomes, S. M. Gomes, O. Mendes, B. Di Pierro, and K. Schneider. Extended generalized lagrangian multipliers for magnetohydrodynamics using adaptive multiresolution methods. *ESAIM Proceedings*, vol. 43, 95–107, (2013).
- [3] M. O. Domingues, S. M. Gomes, O. Roussel, and K. Schneider. Space-time adaptive multiresolution techniques for compressible euler equations. In *The Courant–Friedrichs–Lewy (CFL) Condition: 80 Years After Its Discovery*, Springerlink: Bucher. Birkhäuser Boston, 101–117, (2013).
- [4] A. Frank, T. W. Jones, D. Ryu, and J. B. Gaalaas. The magnetohydrodynamic Kelvin-Helmholtz instability: A two-dimensional numerical study. *The Astrophysical Journal*, vol. 460, 777–793, (1996).
- [5] B. Fryxell, K. Olson, P. Ricker, F. X. Timmes, M. Zingale, D. Q. Lamb, P. MacNeice, R. Rosner, J. W. Truran, and H. Tufo. FLASH: An Adaptive Mesh Hydrodynamics Code for Modeling Astrophysical Thermonuclear Flashes. *The Astrophysical Journal Supplement Series*, vol. 131, 273–334, (2000).
- [6] A. K. F. Gomes. Análise multirresolução adaptativa no contexto da resolução numérica de um modelo de magnetohidrodinâmica ideal. *Dissertação de Mestrado em Computação Aplicada*, Instituto Nacional de Pesquisas Espaciais (INPE), (2012).
- [7] A. K. F. Gomes, M. O. Domingues, K. Schneider, O. Mendes, and R. Deiterding. An adaptive multiresolution method for ideal magnetohydrodynamics using divergence cleaning with parabolic-hyperbolic correction. *Applied Numerical Mathematics*, vol. 95, 199–213, (2015).
- [8] A. Harten. Multiresolution representation of data: a general framework. *SIAM Journal of Numerical Analysis*, vol. 33(3), 385–394, (1996).
- [9] A. Mignone and P. Tzeferacos. A second-order unsplit Godunov scheme for cell-centered MHD: The CTU-GLM scheme. *Journal of Computational Physics*, vol. 229(6), 2117–2138, (2010).
- [10] T. Miyoshi and K. Kusano. A multi-state HLL approximate Riemann solver for ideal magnetohydrodynamics. *Journal of Computational Physics*, vol. 208, 315–344, (2005).
- [11] K. G. Powell, P. L. Roe, T. J. Linde, T. I. Gombosi, and D. L. De Zeeuw. A Solution-Adaptative Upwind Scheme for Ideal Magnetohydrodynamics. *Journal of Computational Physics*, vol. 154, 284–309, (1999).
- [12] O. Roussel, K. Schneider, A. Tsigulin, and H. Bockhorn. A conservative fully adaptive multiresolution algorithm for parabolic PDEs. *Journal of Computational Physics*, vol. 188(2), 493 – 523, (2003).
- [13] E. F. Toro. *Riemann Solvers and Numerical Methods for Fluid Dynamics: A Practical Introduction*. Springer-Verlag Berlin Heidelberg, (1999).